Influence of Topology on the Long-Range Electron-Transfer Phenomenon**

Concepció Rovira,[a] Daniel Ruiz-Molina,[a] Olaf Elsner,[a] Jose Vidal-Gancedo,[a] Jacques Bonvoisin,[b] Jean-Pierre Launay,[b] and Jaume Veciana*[a]

Abstract: Intramolecular electron-transfer phenomena in the radical anions derived from the partial reduction of diradicals (*E*,*E*)-*p*-divinylbenzene-β,β'-ylene bis(4-tetradecachlorotriphenylmethyl) diradical (**1**) and (*E*,*E*)-*m*-divinylbenzene-β,β'-ylene bis(4-tetradecachlorotriphenylmethyl) diradical (**2**) have been studied by optical and ESR spectroscopy. The synthetic methodology used allows for complete control of the geometry of diradicals **1** and **2**, which have *para* and *meta* topologies, respectively, as well as of their *E*/*Z* isomerism. This fact is used to show the influence of the different topologies on the ease of electron transfer, which is larger for the *para* than for the *meta* isomer, in which a small or negligible electronic coupling is observed. A related monoradical compound (*E*)-bis-(pentachlorophenyl)[4-(4-bromophenyl-β-styryl)-2,3,5,6-tetrachlorophenyl]-methyl radical (**3**), which has only one such redox site, has also been obtained and studied for comparison purposes.

Keywords: electron transfer · mixed-valent compounds · organic radicals · radical ions

Introduction

In the last few years, considerable interest has been shown in the study of long-range intramolecular electron-transfer (IET) phenomena in systems formed by donor and acceptor units covalently attached by a rigid organic bridge.[1] The interest arises from the potential use of such systems as molecular wires on integrated molecular-sized devices[2] and, from a theoretical point of view, in studying the roles of the various parameters that govern the intramolecular electron-transfer rate. These studies could give new insights into natural processes such as photosynthesis and allow the rules for the prediction and control of electron propagation in molecular wires to be worked out.[3] Mixed-valence compounds with at least two redox sites that have different oxidation states and are linked by a bridge that mediates the transfer of electrons from one site to the other are excellent candidates for such studies, since intramolecular electron-transfer phenomena can be monitored easily by the study of intervalence transitions. Indeed, the electronic interaction between the two redox sites is characterized by the electronic coupling parameter (V_{ab}), which has the dimension of energy, and can be obtained from the position, intensity, and width of the intervalence transition band, which generally occurs in the near infrared.[4]

Most of the mixed-valence complexes that have been shown to exhibit intervalence transitions are homo- and heterodinuclear metallic complexes in which two metal atoms with different oxidation states are connected through an organic bridging ligand. In contrast, purely organic mixed-valence compounds have so far received only limited attention, probably owing to their high instability.[5] These compounds are characterized by a high delocalization of the electron involved in the intervalence transition along the molecular skeleton, although the role of such a delocalization is still not completely understood. A prime objective of our research has been the synthesis and characterization of purely organic analogues of mixed-valence complexes by using polychlorinated triphenylmethyl radical units. Such radicals are particularly interesting, not only because they have a large persistency, displaying high thermal and chemical stabilities, but also because they are electroactive species that give rise, either chemically or electrochemically, to the corresponding anions and cations which are also quite stable species.[6] As a consequence, we thought it would be interesting to obtain and

[a] Prof. J. Veciana, Dr. C. Rovira, Dr. D. Ruiz-Molina, Dr. O. Elsner, Dr. J. Vidal-Gancedo
Institut de Ciència de Materials de Barcelona (CSIC)
Campus Universitari de Bellaterra, 08193-Cerdanyola (Spain)
Fax: (+34) 93-5805729
E-mail: vecianaj@icmab.es

[b] Dr. J. Bonvoisin, Prof. J.-P. Launay
Molecular Electronics Group, CEMES-LOE/CNRS,
29 rue Jeanne Marvig, B.P. 4347, 31055 Toulouse Cedex 4 (France)

** Generation and Study of Nanometric Organic Mixed-Valence Systems Derived from Triarylmethyl Diradicals. Part 1.

0947-6539/01/0701-0240 $ 17.50+.50/0

study symmetrical molecules that consist of two of these radicals linked by different types of bridges. These diradicals could be converted by a partial reduction (or oxidation) to the corresponding radical anion (or radical cation), and the resulting mixed-valence species would therefore display interesting long-range electron-transfer phenomena. Such phenomena were observed, prior to this work, in a purely organic compound composed of three such triphenylmethyl units covalently connected to an organic bridge.[7]

In order to maximize the electron-transfer rates in mixed-valence compounds, the choice of the bridge is crucial. Both its electronic structure and the effective distance between the redox centers are known to play a critical role in determining the ease of electron transfer. For these reasons, we designed two structurally well-defined diradicals that incorporate phenylene/vinylene units as bridges. The objective was two-fold. Firstly, such spacers give rise to structures in which the extended π conjugation ensures the existence of a long-range electronic coupling between the terminal radicals.[8] Indeed, prior to this work, homo- and heteronuclear metallic complexes with phenylene and/or vinylene units that promoted through-bond, photo-induced energy or electron transfer over considerable distances (i.e., 20 Å) have already been described.[9] Secondly, phenylene and vinylene units allow the construction of series of compounds in which the distance between the active components, as well as the connectivity, can be gradually varied. Moreover, the high degree of rigidity of these spacers avoids any through-space electron transfer during thermally induced encounters between both sides of the molecule.[10]

This paper is devoted to the study, by optical and ESR spectroscopy, of the intramolecular electron-transfer phenomena in the radical anions derived from the partial reduction of pure organic diradicals **1** and **2**.

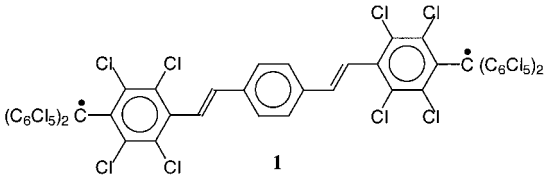

1

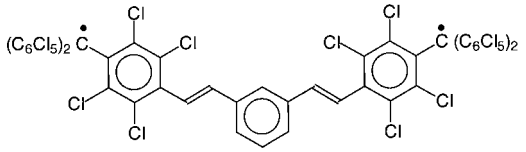

2

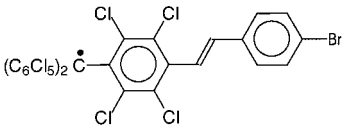

3

These diradicals, which exhibit a defined topology and isomerism, consist of two polychlorinated triphenylmethyl radicals linked by divinylphenylene bridges.[11] The divinylphenylene bridge is expected to be very efficient in transmitting the electronic interaction, as was previously shown in binuclear ruthenium- and osmium-based bis-terpyridyl complexes.[12] In addition, the synthetic methodology used allows complete control of the *E*/*Z* isomerism of diradicals **1** and **2**, which have *para* and *meta* topologies, respectively. We will show that the topology clearly influences the ease of electron transfer. Indeed, small or negligible V_{ab} coupling is expected to appear when the triphenylmethyl radical units are connected in the *meta* position, in contrast to when the two units are in the *para* position. Finally, the related monoradical compound **3**, which has only one such redox site, has also been obtained and studied for comparison purposes.

Results and Discussion

Synthesis: The synthetic route for preparing radicals **1**–**3** is based on two main steps. The first step is the synthesis of their

Abstract in Catalan: *Es presenta l'estudi de fenòmens de transferència electrònica mitjançant espectroscòpies òptiques i de RPE en anions radicals procedents de la reducció parcial dels biradicals (E,E)-p-divinilbenzè-β,β′-ilè bis[4-tetradecaclorotrifenilmetil] (**1**) i (E,E)-m-divinilbenzè-β,β′-ilè bis[4-tetradecaclorotrifenilmetil] (**2**). La metodologia sintètica emprada permet tenir un control complet de la geometria dels biradicals **1** i **2**, els quals presenten topologies para i meta, respectivament, com també de la seva isomeria E/Z. Aquest fet s'utilitza per mostrar l'influència de les diferents topologies en la capacitat de transferència electrònica, la qual es major per l'isòmer para que pel meta, pel qual s'observa un acoblament electrònic molt feble o negligible. Per raons comparatives, també s'ha obtingut el compost monoradicalari (E)-bis(pentaclorofenil)[4-(4-bromofenil-β-estiril)-2,3,5,6-tetraclorofenil]-metil (**3**), el qual només presenta un centre redox.*

Abstract in French: *Le transfert électronique intramoléculaire dans les radicaux anions obtenus par réduction partielle des biradicaux (E,E)-p-divinylbenzène-β-β′-yléne bis[4-tetradécachlorotriphénylméthyl] (**1**) et (E,E)-m-divinylbenzène-β-β′-ylène bis[4-tetradécachlorotriphénylméthyl] (**2**) a été étudié par spectroscopies optique et RPE. La méthodologie synthétique utilisée permet un contrôle complet de la géométrie des biradicaux **1** et **2**, qui présentent les topologies para et méta respectivement, ainsi que de leur isomérie Z/E. Ceci est utilisé pour montrer l'influence des différentes topologies sur la facilité du transfert d'électron, qui se révèle plus grande pour l'isomère para que pour le méta, ce dernier ne présentant qu'un couplage électronique faible ou négligeable. Enfin un monoradical apparenté, le (E)-bis(pentachlorophényl)[4-(4-bromophényl-β-styryl)2,3,5,6-tétrachlorophényl]méthyl (**3**), qui ne présente qu'un site redox de ce type, a aussi été obtenu et étudié aux fins de comparaison.*

triphenylmethane precursors by a Wittig reaction, while the second step is the generation of the corresponding mono- or dicarbanion by an acid–base reaction, followed by the subsequent oxidation of such carbanions to the corresponding mono- or diradical.

Treatment of the bromomethane derivative **4**,[13] with triphenylphosphine yielded the substituted phosphonium bromide **5** (Scheme 1). This was coupled with *p*-bromobenzaldehyde by a Wittig reaction to give the corresponding

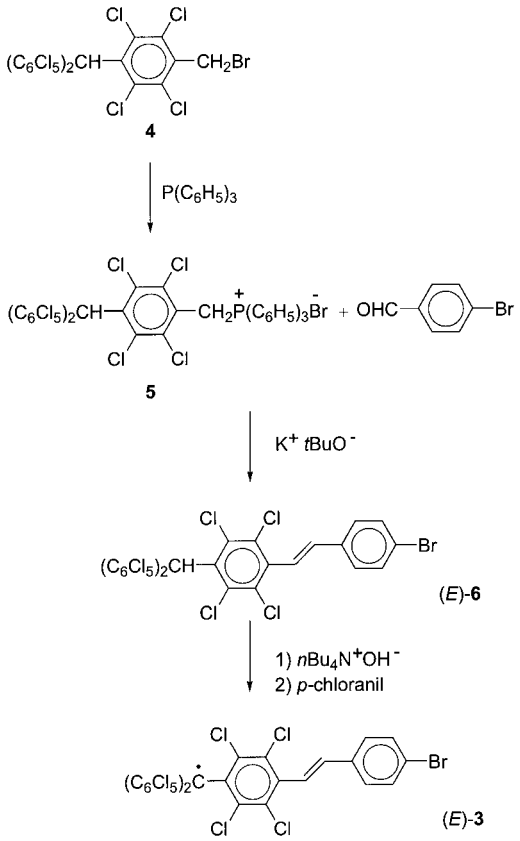

Scheme 1.

polychlorinated triphenylmethane (*E*)-**6**, which is the precursor of radical (*E*)-**3**. This reaction is strongly stereoselective, since it yields exclusively the *E* isomer.[14] Such stereoselectivity is explained by considering that the ylide derived from the phosphonium bromide **5** is stabilized by the presence of the polychlorinated aromatic ring. Indeed, it has been shown experimentally that, with electron-withdrawing groups which stabilize the betaine form, the natural preference of ylides is to give mainly the *E* isomer.[15] The *Z*/*E* isomer distribution of the Wittig products is also strongly influenced by the nature of the base used in the preparation of the ylide;[16] in this case potassium *tert*-butoxide—the base of choice for maximizing the yields of *E* olefins.[17] Finally, the synthesis of the monoradical (*E*)-**3** was undertaken by treating the triphenylmethane precursor (*E*)-**6** with an excess of nBu$_4$N$^+$OH$^-$ and subsequent oxidation of the resulting anion with *p*-chloranil in a one-pot reaction. Remarkably, the resulting radical species retained the *E* configuration of its precursor in spite of the use of a strong base and an oxidizing agent.

The *E* configuration of radical **3** and its precursor **6**, was experimentally confirmed by preparing mixtures of the *Z* and *E* isomers of both compounds. With this aim, the Horner–Emmons coupling reaction of *p*-bromobenzaldehyde with phosphonate **7** was carried out.[18] The substituted phosphonate **7** was obtained by treating the bromomethane derivative **4** with an excess of triethylphosphite (Scheme 2). The reaction of **7** with *p*-bromobenzaldehyde in the presence of potassium *tert*-butoxide then yielded a mixture of the (*E*)-**6** and (*Z*)-**6** isomers. Both isomers were isolated by chromatography and unequivocally assigned by FTIR and ^{1}H NMR spectroscopy. The isolation of both isomers also allowed us to obtain the radicals (*E*)-**3** and (*Z*)-**3** by treatment of the triphenylmethanes (*E*)-**6** and (*Z*)-**6**, respectively, with an excess of nBu$_4$N$^+$OH$^-$ and subsequent oxidation of the resulting anions with *p*-chloranil. It must be emphasized that the chromatographic retention indexes and the spectra of (*E*)-**3** and (*E*)-**6** were in excellent agreement with those obtained for the compound resulting from the Wittig reaction and its corresponding radical; this confirmed the stereoselectivity of the last reaction.

Diradicals **1** and **2** were prepared by following a similar procedure. As shown in Scheme 3, the phosphonium bromide **5** was coupled with *p*-phthaldehyde and *m*-phthaldehyde by a bis-Wittig reaction to give the bistriphenylmethane derivatives **8** and **9**, respectively. It must be emphasized that the bis-Wittig reaction is also strongly *E,E* selective, as spectroscopically ascertained.

Afterwards, the synthesis of the diradical species **1** and **2** was undertaken by treating the corresponding triphenylmethane precursors **8** and **9** with an excess of nBu$_4$N$^+$OH$^-$ and subsequent oxidation of the resulting dianions with *p*-chloranil in a one-pot reaction. Diradicals **1** and **2** were isolated as dark brown (75%) and green (68%) solids, respectively, and were characterized as the *E,E* isomers. As described for the monoradical (*E*)-**3**, no isomerization of double bonds was noticed for either diradical by spectroscopic

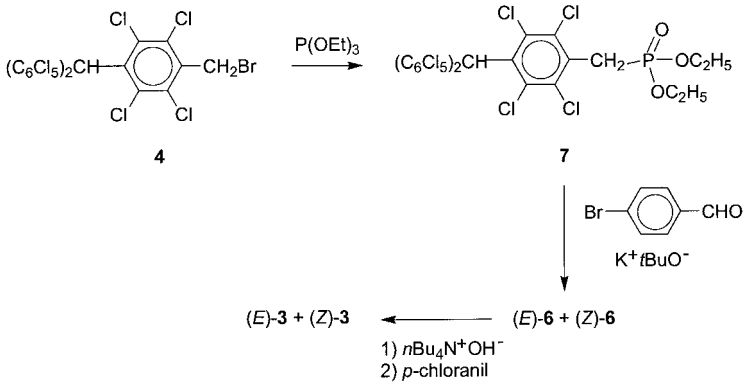

Scheme 2.

0947-6539/01/0701-0242 $ 17.50+.50/0 *Chem. Eur. J.* **2001**, *7*, No. 1

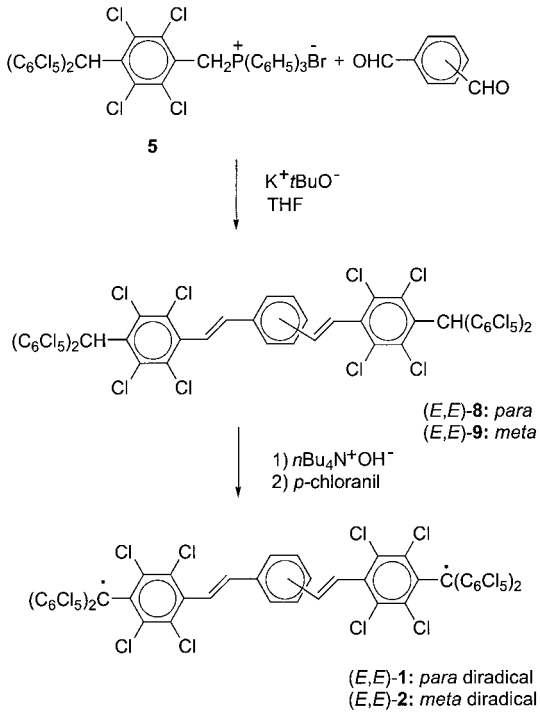

Scheme 3.

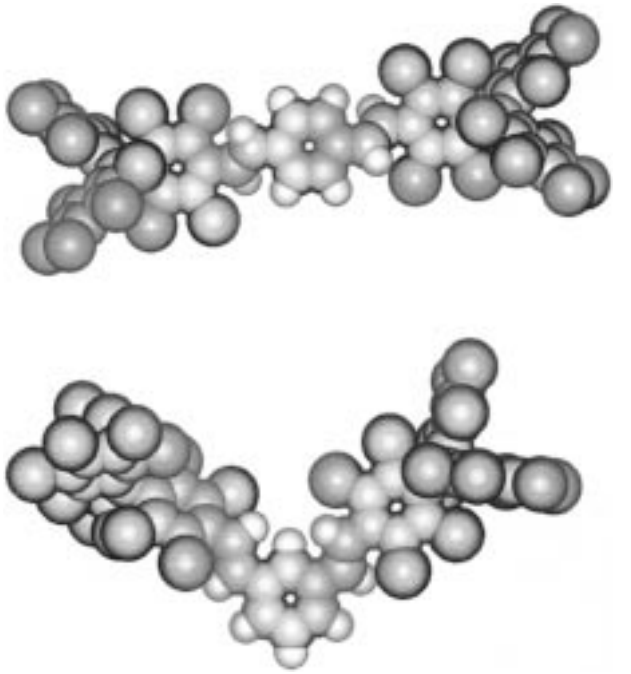

Figure 1. AM1 semiempirical optimized structure of diradical **1** (top) and diradical **2** (bottom).

techniques. Finally, it is worth noting that both diradicals are highly persistent and thermally stable in the solid state and also in diluted solutions, even when exposed to air. No enhanced reactivities of the diradicals with respect to their monoradical counterparts were observed.

Physicochemical characterization: Semiempirical AM1 calculations were performed to explore the geometry and the conformation of diradicals **1** and **2** around the vinylene bridges and their possible influence in the IET (intramolecular electron-transfer) processes.[19] The resulting minimized geometries for the *para* and *meta* isomers are shown in Figure 1. The AM1-optimized structure of diradical **1** has an extended S-shaped profile, whereas that of diradical **2** has a U-shaped profile. The origin of such different profiles is the different topological *para* and *meta* substitution of the divinylphenylene bridge; this results in a significantly larger through-space distance between the two electron active sites[20] in diradical **1** (18.7–18.9 Å) than in **2** (15.1–16.9 Å).

In the case of the *para* isomer, the degrees of twist of the inner aromatic group of the triphenylmethyl units, with respect to their adjacent vinylene moiety, are 45° and 52°; this deviates strongly from coplanarity. In addition, the two vinylene moieties are bent and twisted out of the plane defined by the central p-phenylene ring. Indeed, the dihedral angles between the two vinylene moieties and the central p-phenylene ring are 44° and 50°. Similar deviations from coplanarity were observed for the *meta* isomer. In this case, the degrees of twist of the inner aromatic group of each triphenylmethyl unit with respect the plane defined by the vinylene moieties are 40° and 60°, and the dihedral angles between the two vinylene moieties and the central *m*-phenylene ring are 45° and 52°. The fact that the phenylene, vinylene, and triphenylmethyl units are severely twisted in relation to each other confirmed the lack of effective conjugation in these polyaromatic systems. The absence of effective conjugation seems to be common to most of the oligomers so far described in the literature, and especially to other vinylene-phenylene-vinylene-bridged redox systems. For instance, the solid-state structure of a bis-octamethylferrocenyl complex, bridged by one of the aforementioned units, showed that the vinylene, phenylene, and cyclopentadienyl subunits are twisted in relation to each other with torsion angles of 21° and 13°.[21]

It must be noted that, as far as intramolecular electron-transfer phenomena are concerned, the main distance to be considered is the through-bond distance between the two electron active sites;[20] that is, the sum of bond lengths corresponding to the conjugated pathway. These distances, measured from one radical alpha-carbon atom to the other, are 24.1 and 22.7 Å for diradicals **1** and **2**, respectively. However, as will be shown later on by ESR spectroscopy, the average distance between the two spins—the average inter-spin separation—in both diradicals differs from the nominal separation, either through-space or through-bond between the two radical alpha-carbon atoms obtained from the AM1 minimized structures, owing to the different extent of the delocalization in the diradicals.

Electrochemical studies in CH_2Cl_2, with nBu$_4$NPF$_6$ (0.1M) as supporting electrolyte (vs SCE) and a Pt wire as a working electrode, were done at room temperature. In the cyclic voltammogram (CV) of monoradical **3** only one reduction process was observed at a potential of -0.32 V (vs. SCE). The presence of only one reduction process is in accordance with the presence of a unique, electrochemically active, chlorinated triphenylmethyl unit. The CV of diradicals **1** and **2** also show only one reversible reduction process at a constant potential of approximately -0.23 V (vs SCE), in spite of the presence

of two electronically active triphenylmethyl units. This result suggests the presence of very weak or negligible electronic interactions between the triphenylmethyl units of diradicals **1** and **2**, since in the case of a strong or moderate electronic interaction between the two units, two electrochemical waves would be anticipated. Only if both units exhibit very weak or negligible electronic interactions, would the two standard redox potentials be very close and a single two-electron wave be observed, with minor differences in shape compared with a true bielectronic process. The cyclic-voltammetric peak separations of the reversible reduction waves for diradicals **1** and **2** are 83 and 78 mV, respectively; this is similar to what is observed for the monoradical **3** (80 mV). Such separation is one criterion for electrochemical reversibility and the separation observed for radicals **1**–**3** is close to the expected theoretical value of 59 mV. The slightly higher peak separation may arise from the high resistance of the solutions used for the measurements.

The magnetic susceptibility of powder samples of radicals **1**–**3** was measured over a temperature range of 4–300 K. The χT versus T plot of radical **3** gives a straight line down to low temperatures, at which point a small downward deviation is observed.[22] This deviation can be described by the Curie–Weiss law with a θ of -0.6 K, which indicates the presence of weak intermolecular antiferromagnetic interactions. The effective magnetic moment found at room temperature (1.69 μ_B) was in agreement with that expected for a compound with only one unpaired electron (1.73 μ_B). Diradicals **1** and **2** also follow the Curie–Weiss law, down to low temperatures, with θs of -4 K and -0.4 K, respectively, owing to weak intra- and/or intermolecular antiferromagnetic interactions. The effective magnetic moments found at room temperature were 2.41 and 2.43 μ_B for diradicals **1** and **2**, respectively. These values are in excellent agreement with the theoretical effective magnetic moment expected for a noninteracting pair of doublets (2.45 μ_B).

UV-visible spectra of diradicals **1** and **2** were recorded and compared with those obtained for the analogous monoradical **3**. Relevant data are shown in Table 1. Visible spectra of polychlorotriphenylmethyl radicals usually show an intense absorption band at 386 nm and two weaker bands centered around 565–605 nm, all of which are assigned to the radical character of the triphenylmethyl units.[6] In the case of radicals **1**–**3**, owing to the presence of a certain degree of electronic delocalization, bathochromic shifts with enhanced absorptivities compared with unsubstituted chlorinated triarylmethyl radicals would be expected. This behavior is indeed observed for monoradical **3** and diradical **2**, which show similar absorption positions although with approximately double absorptivity values for the latter, owing to the presence of two apparently noninteracting radical centers. By contrast, for diradical **1**, substantially larger bathochromic shifts and enhanced absorptivities are observed, as expected from the larger electronic delocalization present in this compound owing to its *para* connectivity.

X-band ESR spectra of radicals **1**–**3** were obtained in CH_2Cl_2 over a temperature range of 180–293 K. The isotropic ESR spectra at 300 K were fairly well simulated by using the parameters given in Table 1. The experimental and simulated spectra of radicals **1** and **3** are given in Figure 2 for comparison purposes. The spectra of radicals **1**–**3** at room temperature had lines corresponding to the coupling of the unpaired electrons with the different nuclei of nonzero magnetic moments, that is, with ^{1}H and the naturally abundant ^{13}C nuclei. Computer simulation gave the isotropic g values (g_{iso}) and the isotropic hyperfine-coupling constants (a_i). The g_{iso} values obtained were 2.0022, 2.0024, and 2.0028 for radicals **1**, **2**, and **3**, respectively, and are very close to those

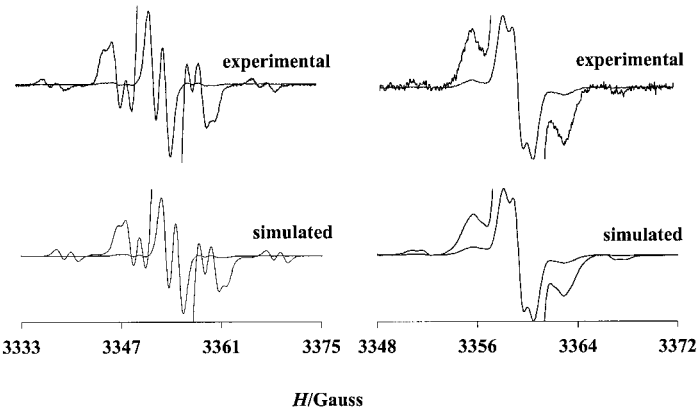

Figure 2. Simulated and experimental isotropic-solution EPR spectra of radicals **1** (right) and **3** (left) in CH_2Cl_2 at 200 K.

Table 1. Relevant UV/Vis and ESR data.

	ESR[a,b]						UV/Vis[e]
	$\Delta H_{1/2}$	a_H	$a_{C\alpha}$	a_{Carom}	D/hc	E/hc	λ [nm] ($\varepsilon \cdot 10^{-3}$)
1	0.95	0.95 (2H)	14.0	5.9, 6.4	$3.9 \cdot 10^{-4}$	[c]	600(3.2), 440(20.7), 386(57.4), 339(33.1)
1$^{\bullet-}$	0.85	1.90(1H)	[d]	[d]	–	–	[f]
1^{2-}	–	–	–	–	–	–	606(46.4), 522(49.3), 339(32.3)
2	0.98	0.90(2H)	13. 9.0	5.5, 6.5	$2.3 \cdot 10^{-4}$	[c]	573(3.1), 415(26.0), 385(33.7)
2$^{\bullet-}$	0.58	1.80(2H) 0.60 (2H)	[d]	[d]	–	–	[f]
2^{2-}	–	–	–	–	–	–	570(49.4), 525.4(51.4), 293(39.2)
3	1.00	1.80(1H)	29.5	10.7, 13.0	–	–	567(1.5), 430(15.9), 386(28.2), 295(22.4)
3$^-$	–		–	–	–	–	570(22.9), 525(22.6), 301(18.3)

[a] In CH_2Cl_2 solutions at RT; except for **1**$^{\bullet-}$ and **2**$^{\bullet-}$ which were taken at 200 K. [b] Line widths and hyperfine-coupling constants (in Gauss) are computer-simulated values, the g values found were similar, 2.0027(3), for all open-shell species. Zero-field splitting parameters (in cm^{-1}) observed in frozen solutions at 120 K. Principal components of g tensors for **1**$^{\bullet-}$ and **2**$^{\bullet-}$ are $g_x = 2.0033$, $g_y = 2.0033$, $g_z = 2.0010$ and $g_x = 2.0029$, $g_y = 2.0029$, $g_z = 2.0025$, respectively. These values were determined by simulation of frozen ESR spectra. [c] Negligible. [d] Not observed. [e] In CH_2Cl_2 solution at RT. [f] See text.

0947-6539/01/0701-0244 $ 17.50+.50/0 *Chem. Eur. J.* **2001**, *7*, No. 1

observed for other polychlorotriphenylmethyl radicals.[6] More interesting is the comparison of the values of the isotropic hyperfine-coupling constants with those of the hydrogen nuclei of the vinylene moieties and with those of some of the carbon nuclei of the triphenylmethyl unit. For instance, the ESR spectrum of radical **3** at 300 K displays two main symmetrical lines caused by hyperfine coupling with one hydrogen atom of the ethylene moiety, whereas, in the case of diradicals **1** and **2** three lines are observed. Moreover, the values of the coupling constants for diradicals **1** and **2** are approximately half that of those found for monoradical **3**. It is then possible to conclude that the two electrons in diradicals **1** and **2** are interacting magnetically, with a magnetic exchange coupling constant J that fulfills the following condition: $J \gg a_i$.

The absolute values of zero-field splitting parameters, $|D/hc|$ and $|E/hc|$, for diradicals **1** and **2** were obtained from the simulated spectra of both diradicals in frozen $CFCl_3$ and are given in Table 1. These parameters arise from the dipolar magnetic interactions between the two unpaired electrons and can be used to calculate the average interspin separation in a given compound. Therefore, from the zero-field splitting parameter $|D/hc|$ in cm^{-1} and Equation (1),[23] an average interspin separation of 19 or 22 Å was found for diradicals **1** and **2**, respectively.

$$r = \left[\frac{3g^2\beta^2}{2hc}\,\frac{1}{|D/hc|}\right]^{1/3} \qquad (1)$$

The average interspin separation found for diradical **1** is smaller than the nominal separation between the two alpha carbon atoms (vide supra) where most of the spin density of polychlorinated triphenylmethyl radicals is localized. This result is in agreement with the existence of a certain degree of electronic delocalization owing to the *para* connectivity of the divinylphenylene bridge that reduces the effective separation of the two spins in **1**. As expected, the average interspin separation found for diradical **2** is much closer to the nominal separation between the two alpha carbon atoms owing to the lower degree of electronic conjugation in the *meta* isomer relative to the isomer with *para* connectivity. Finally, ESR measurements of frozen dilute solutions of both diradicals over a 4–100 K range revealed that a very weak magnetic interaction exists between the two unpaired electrons, since the signal intensity for both diradicals follows Curie's law. This result, along with the $J \gg a_i$ condition, permits the limits for the intramolecular exchange coupling constant for diradicals **1** and **2** to be estimated, that is $15\ cm^{-1} \gg J/hc \gg 10^{-3}\ cm^{-1}$.

Intramolecular electron-transfer process: Determination of the experimental electronic coupling parameter V_{ab} has been undertaken by spectroelectrochemistry by using a previously described methodology.[24] This methodology is based on the reduction of diradicals **1** and **2** and the simultaneous observation of the corresponding electronic absorption spectra, regularly recorded during the reduction process for different values of the average number of electrons added (n) such that $0 \le n \le 2$. This situation allows the evolution of the electrochemical reaction to be controlled simply by monitoring the evolution of the characteristic radical and anion bands. The different reduced species that can be derived from both diradicals are depicted schematically in Scheme 4. As can be seen here, diradicals **1** and **2**, as well as the dianion $\mathbf{1}^{2-}$ and $\mathbf{2}^{2-}$, are homovalent species, whereas the radical anions $\mathbf{1}^{\bullet-}$ and $\mathbf{2}^{\bullet-}$ should be regarded as a mixed-valence species. Thus, only the last species may show intervalence transition bands that usually appear at low energies, that is, in the near-infrared region.

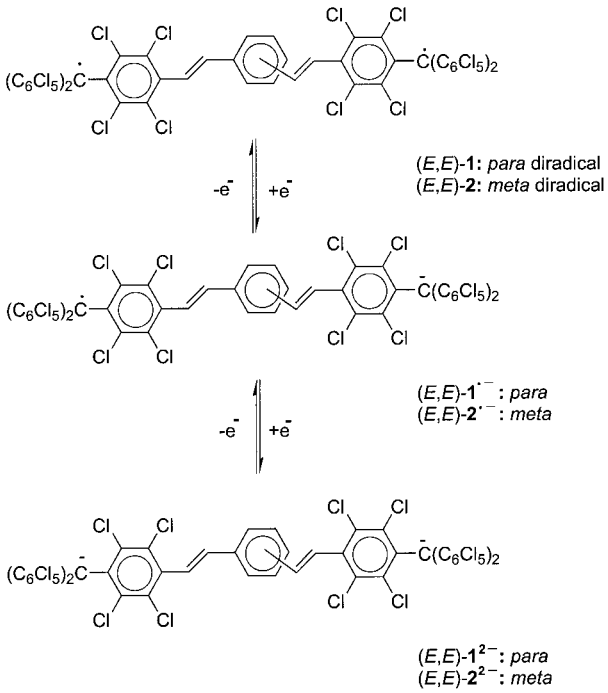

Scheme 4.

During the reduction of diradical **1**, the sharp band at 386 nm, characteristic of the radical chromophore, decreases until it completely disappears for $n = 2$, while the band at 339 nm does not change at all. At the same time, two new broad and intense bands grow at 522 and 606 nm; these correspond to the continuous formation of the dianion $\mathbf{1}^{2-}$. Similar behavior was observed for diradical **2**. During the reduction process, the sharp, intense band centered at 385 nm decreases progressively until it completely disappears for $n = 2$. Simultaneously, two new broad and intense bands grow at 525 and 570 nm, characteristics of the dianion $\mathbf{2}^{2-}$. The evolution of the UV-visible spectra during the course of the reduction of diradical **2** is shown in Figure 3. The observation of some well-defined isosbestic points during reduction of diradicals **1** and **2** indicates that no by-products are generated by decomposition processes during such electrochemical reductions.

The main difference in the stepwise coulometric titration of diradicals **1** and **2** is the observation of a new band centered at 1400 nm for the radical anion $\mathbf{1}^{\bullet-}$, shown in Figure 4. Indeed, during the reduction process of diradical **1**, a weak, broad band centered at 1400 nm appears and develops until the complete formation of $\mathbf{1}^{\bullet-}$. Afterwards, the intensity of this band decreases until it disappears when the dianion $\mathbf{1}^{2-}$ is completely formed. This is the typical behavior expected for

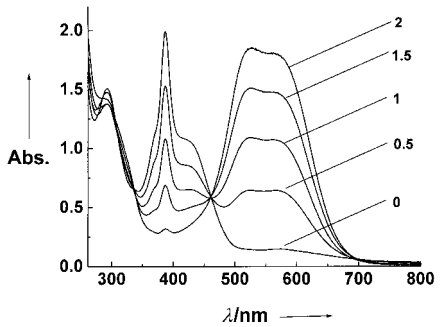

Figure 3. Evolution of the UV/Vis spectrum during the course of the reduction of diradical **2**. The number of added electrons is given on each spectrum.

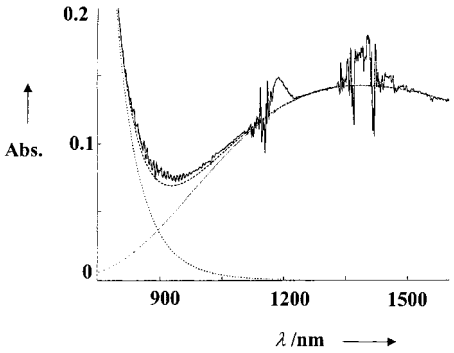

Figure 4. Corrected electronic spectra for the mixed-valence species $\mathbf{1}^{\bullet-}$: (——) experimental spectrum; (- - - -) simulated spectrum = sum of the intervalence transition band (– – –) and the transition band corresponding to the radical and/or anion chromophore (· · ·). The two bands at 1200 and 1350 nm are artifacts due to solvent absorption.

an intervalence band caused by the presence of an intramolecular electron-transfer phenomenon in the mixed-valence species $\mathbf{1}^{\bullet-}$. On the other hand, no intervalence band at 1400 nm, or even at larger or smaller wavelengths, was detected for the radical anion $\mathbf{2}^{\bullet-}$ formed during the reduction of diradical **2**.

Optically activated electron-transfer process in $\mathbf{1}^{\bullet-}$: The assignment of the band centered at 1400 nm as an intervalence transition was confirmed by theoretical calculations following the method previously employed by Nelsen et al.[25] The energy of an intervalence transition (λ) comes from two different contributions, λ_{in} and λ_{out}, which correspond to the energy contributions produced by the arrangements of the internal part of the system (the molecule) and the outer medium (the solvating medium), respectively, when the electron is transferred. The inner shell term, or internal Marcus term, for polychlorinated triphenylmethyl radicals, $\lambda_{in} = 0.214$ eV, was obtained by quantum mechanical calculations at the AM1 level performed on the $(C_6Cl_5)_3C^{\bullet}$ fragment.[26] The outer shell term was estimated using the Marcus dielectric continuum model shown in Equation (2).

$$\lambda_{out} = 14.41\, g(r,R)\gamma \qquad (2)$$

Here γ is the Marcus solvent parameter, which is 0.380 for CH_2Cl_2, $g(r,R)$ is the geometrical parameter of the electron active center and λ_{out} is given in eV. The $g(r,R)$ parameter is calculated from the effective radius, r, of the localized charge—represented as a sphere centered at the carbon atom—and R, the distance between the centers of the two electron active centers by using Equation (3).

$$g(r,R) = \frac{1}{r} - \frac{1}{R} \qquad (3)$$

With $r = 5.4$ Å, determined from the X-ray structure of the $(C_6Cl_5)_3C^{\bullet}$ radical,[6e] and $R = 19$ Å as the limit distance between the two electron active sites, vide supra, one obtains $\lambda_{out} = 0.726$ eV. Summation of both contributions yields $\lambda = 0.939$ eV, which is in fairly good agreement with the experimental value of 0.787 eV, vide infra, determined from the position of the intervalence band. Interestingly, λ_{in} provides a noteworthy contribution to the total energy of the intervalence transition λ here, whereas in the related case of partly oxidized tertiary aromatic amines this term was almost negligible relative to λ_{out}.[5d]

In order to determine the effective electronic coupling V_{ab} (in cm^{-1}) between the redox sites of diradical **1** experimentally, we can use Equation (4), developed by Hush.

$$V_{ab} = [2.05 \times 10^{2-} \sqrt{\varepsilon_{max}\bar{\nu}_{max}\Delta\bar{\nu}_{1/2}}]R^{-1} \qquad (4)$$

Here V_{ab} is given in cm^{-1}, R is the effective separation of the redox sites (in Å), ε_{max} is the maximum extinction coefficient (in $M^{-1}cm^{-1}$), $\bar{\nu}_{max}$ is the transition energy, and $\tilde{\nu}_{1/2}$ is the full-width at half-height (both in cm^{-1}) of the intervalence absorption band. After correction for the comproportionation equilibrium between the different redox forms of **1**, $\mathbf{1}^{\bullet-}$, and $\mathbf{1}^{2-}$, and the deconvolution of the experimental spectrum,[27] the following parameters for the intervalence absorption band were obtained: $\tilde{\nu}_{max} = 6349\ cm^{-1}$ (i.e. $\lambda = E_{opt} = 0.787$ eV), $\Delta\tilde{\nu}_{1/2} = 2940\ cm^{-1}$, and $\varepsilon_{max} = 677\ M^{-1}cm^{-1}$. Application of these parameters to Equation (4) provides an effective electronic coupling for $\mathbf{1}^{\bullet-}$ of $V_{ab} = 121\ cm^{-1}$ (0.015 eV), when $R = 19$ Å is used.

Thermally activated electron-transfer processes: The electron transfer in $\mathbf{1}^{\bullet-}$ was also studied by ESR spectroscopy. For this purpose, the electrochemical reduction of **1** was performed until an almost complete reduction to $\mathbf{1}^{2-}$ was achieved. Besides the desired mixed-valence species $\mathbf{1}^{\bullet-}$, the resulting solution mainly contained the EPR-silent species $\mathbf{1}^{2-}$ and, therefore, the resolution of the spectra is good. The ESR spectrum of $\mathbf{1}^{\bullet-}$ at 200 K displays two symmetrical lines (Figure 5) with an ^1H hyperfine-coupling constant very close to that of the monoradical **3** (Table 1). This result clearly demonstrates that, at this temperature and on the ESR timescale, the unpaired electron of radical anion $\mathbf{1}^{\bullet-}$ is localized on only one-half of the molecule, that is, on one stilbene-like moiety.

As depicted in Figure 5, when the temperature is increased, a new central line gradually emerges between the two initial ones. This evolution is consistent with the increase of the electron-jump rate on going from 200 K (the slow-exchange limit) to 300 K (the fast-exchange limit), owing to a thermally activated electron transfer between the two equivalent sites; this leads to the coupling of the unpaired electron of $\mathbf{1}^{\bullet-}$ with two equivalent ^1H nuclei. The ESR spectra of $\mathbf{1}^{\bullet-}$ at various

0947-6539/01/0701-0246 $ 17.50+.50/0 *Chem. Eur. J.* **2001**, *7*, No. 1

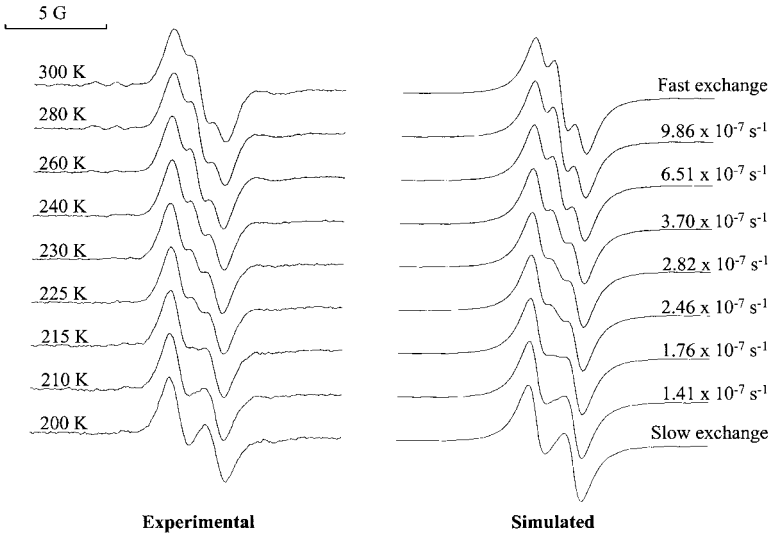

Figure 5. Experimental and simulated ESR spectra of $\mathbf{1}^{\bullet-}$ at different temperatures in CH_2Cl_2 with 0.1M of nBu$_4$NPF$_6$. The spectra were recorded at the very end of the reduction process, at which stage the major species present in the solution is the ESR-silent dianion $\mathbf{1}^{2-}$. Most of the observed ESR signal is due to $\mathbf{1}^{\bullet-}$ since, for statistical reasons, diradical **1** must have negligible concentration. The simulated spectra were performed with ^{1}H(1 H) = 1.90 G, $\Delta H_{1/2} = 0.85$ G, and the electron exchange rate constant given on each spectrum.

temperatures were fairly well simulated by using the rates given in Figure 5 and the Heinzer program.[28] The best fit was made by varying the rate constant k_{th} for the thermally activated electron transfer between the two equivalent sites. The resulting k_{th} values were plotted using a linear Eyring plot [$\ln(k_{th}/T)$ vs. $1/T$] from which a value for the energy barrier to the thermal electron transfer, ΔH^*, of 0.117 eV was obtained.

According to Hush theory, E_{opt} corresponds to the energy for the vertical electron transfer between the sites. As shown in Figure 6, at the limit of a vanishingly small electronic interaction (i.e., $V_{ab} \approx 0$), the thermal barrier to electron transfer is predicted to be one fourth of E_{opt}, because of the usual parabolic shape of the energy wells, according to Equation (5),

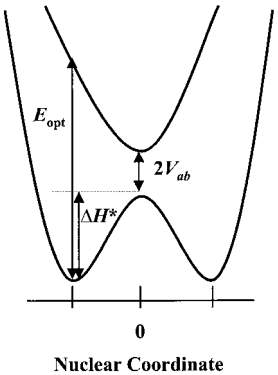

Figure 6. Potential energy curves for the mixed-valence radical anions that can be derived from diradicals **1** and **2**; these represent the system at any geometry along the nuclear coordinate. The electron is vibrationally localized in one of the redox centers owing to the presence of an activation energy barrier (ΔH), although such a barrier may be overcome by an external optical or thermal stimulus to promote an IET process.

$$\Delta H^* = (E_{opt}/4) - V_{ab} \qquad (5)$$

In the present case, this equation is not fulfilled, because ΔH^* (0.117 eV) is appreciably lower than one-fourth of the optical energy (0.787/4 = 0.197 eV). A naïve argument would be to assign the difference to the presence of a significant electronic coupling. This would give $V_{ab} = 0.080$ eV, a value much higher than the one found experimentally from the intensity of the intervalence transition with Equation (4), that is, 0.015 eV. Several hypotheses can be considered to explain the difference in V_{ab} values obtained by both methods: i) The determination of V_{ab} by a difference between two terms of comparable magnitude from Equation (5), is certainly highly inaccurate. ii) Some processes such as nuclear tunneling could contribute to lowering the effective thermal energy barrier. iii) The use of Equation (4) to calculate V_{ab} may not be correct for organic compounds in which there is a certain degree of electronic delocalization. In fact, the separation between the redox sites, R, which is employed in Equation (4), is not perfectly defined because, in the ground state, the wave function of the electron is not fully localized on the alpha carbon atom, but has an important extension onto the adjacent phenyl rings. This fact has already been pointed out by Nelsen et al.[29] and by two of the authors for organic nitrogen compounds.[5d]

The ESR spectrum of $\mathbf{2}^{\bullet-}$ at 200 K has two symmetrical lines, each one with a shoulder, caused by the hyperfine coupling with the hydrogen atoms of the ethylene moiety. The ESR spectrum at 200 K was fairly well simulated by using the parameters given in Table 1. The experimental and simulated ESR spectra are compared in Figure 7. One of the resulting ^{1}H hyperfine-coupling constants is very close to that observed for monoradical **3** and the mixed-valence radical anion species $\mathbf{1}^{\bullet-}$, whereas the second one is considerably smaller. Similar behavior has been observed in other polychlorinated bis(triphenylmethyl) systems.[30] When the temperature is increased no evolution is observed, which confirms that, at least within the temperature range studied, intramolecular electron transfer is not observed because it is slower than the timescale of the ESR experiment. This result, together with the lack of an intervalence band transition in the absorption spectra, suggests that there is a localization effect in the radical-anion species $\mathbf{2}^{\bullet-}$. Previous experimental and theoretical studies performed on diferrocenylbenzenes showed that such localization occurs when the two electroactive centers are con-

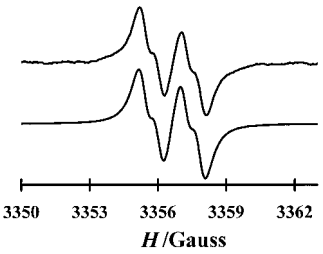

Figure 7. Experimental (top) and simulated (bottom) ESR spectra of the mixed-valence species $\mathbf{2}^{\bullet-}$ in a frozen solution of CH_2Cl_2 at 200 K.

nected in the *meta* position, whereas if they are connected in the *para* position, intramolecular electron transfer across the phenylene ring is observed.[31] Similar results have also been detected in polynorbornyl and divinyl alkane systems. Indeed, recent studies have shown that V_{ab} values are markedly larger for polynorbornyl dienes than for the divinyl alkanes—by as much as 35% for the shorter members and 20% for the larger members. These surprising results indicate that simple *n*-alkyl bridges are more effective mediators of through-bond coupling over long distances than polynorbornyl bridges, even though the chromophore units in the latter are connected by two alkyl relays, rather than one. The authors infer from these results that there is interference between the various coupling pathways in the polynorbornyl bridge.[32]

Conclusion

Diradicals **1** and **2**, which only differ in their topological connectivity, have been synthesized and characterized. The AM1-minimized structures allowed us to evaluate the through-bond and through-space distances between their electron active sites. However, ESR experiments confirmed that the average interspin separation found for diradical **1** is smaller than the nominal separation between the two radical carbon atoms where most of the unpaired electrons are located. On the other hand, the average interspin separation for diradical **2** is very close to the nominal separation between the two alpha C atoms; this suggests a larger electronic localization effect. Such averaged interspin distances are crucial when considering the V_{ab} electronic coupling. Intramolecular electron-transfer phenomena in the mixed-valence radical-anion species $\mathbf{1}^{\bullet-}$ have been observed and studied by a spectroelectrochemical titration and temperature-variable ESR experiments. Interestingly, $\mathbf{1}^{\bullet-}$ constitutes one of the rare examples of a mixed-valence species for which the determination of both the optical and thermal energies for electron transfer is possible.[29] In contrast to $\mathbf{1}^{\bullet-}$, no electron transfer was observed for $\mathbf{2}^{\bullet-}$, a result that can be ascribed to the localization of frontier orbitals in the latter radical anion because of the *meta* connectivity of this non-Kekulé molecule.

Experimental Section

All solvents were reagent grade from SDS and were used as received unless otherwise indicated. All reagents, organic and inorganic, were of high purity grade and obtained from Merck, Fluka, and Aldrich. Elemental analyses were obtained in the Servei de Microanalisi del CID (CSIC), Barcelona.

Direct current (dc) magnetic susceptibility measurements were carried out on a Quantum Design MPMS SQUID susceptometer with a 55 kG magnet and an operating range of 4–320 K. All measurements were collected in a field of 10 kG. Background correction data were collected from magnetic susceptibility measurements on the holder capsules. Diamagnetic corrections, estimated from the Pascal constant, were applied to all data for determination of the molar paramagnetic susceptibilities of the compounds. EPR spectra were recorded on a Bruker ESP-300E spectrometer operating in the X-band (9.3 GHz). The signal-to-noise ratio was increased by accumulation of scans with the F/F lock accessory to guarantee a high-field reproducibility. Precautions were taken to avoid undesirable spectral-line broadening, such as that arising from microwave power saturation and magnetic field over-modulation. To avoid dipolar broadening, the solutions were carefully degassed three times by using vacuum cycles with pure argon. The *g* values were determined against the DPPH (1,1-diphenyl-1-picrylhydrazyl) standard ($g = 2.0035$). Electrochemical experiments were performed with an Electromat 2000 system (ISMP Technologies), by using a platinum wire as working electrode and a saturated calomel electrode (SCE) as reference electrode. Anhydrous CH_2Cl_2 was freshly distilled over P_2O_5 under nitrogen. Commercial tetrabutylammonium hexafluorophosphate (Fluka, electrochemical grade) was used as the supporting electrolyte. UV/Vis and near-IR were recorded with a Shimadzu UV-PC 3101 and a Beckman Acta M VI spectrophotometers. Reductions were performed by electrolysis in a two-compartment cell with CH_2Cl_2 as solvent and 0.1M tetrabutylammonium tetrafluoroborate as supporting electrolyte. The progress of the reduction was followed coulometrically. The ^{1}H NMR spectra were recorded with a Bruker FT80 spectrometer (^{1}H NMR 80 MHz).

The geometries of diradicals **1** and **2** were minimized by using UHF-AM1 semiempirical minimizations.[33] These calculations were performed with the HyperChem 3 molecular modeling package. The initial input geometries (excluding the propeller-like arrangement of each triaryl moiety) were kept planar, that is, the dihedral angles defined by the vinylene moieties and the phenylene rings were set to 0°. Moreover, for each diradical, two different initial input conformations were used, which differed by a 180° rotation around one of the single bonds that connects the central phenylene unit and one of the vinylene moieties,. It is important to note that, independently of the input model used, the minimized geometries converged to similar close-lying minima.

{4-[Bis(2,3,4,5,6-pentachlorophenyl)methyl]-2,3,5,6-tetrachlorobenzyl}(triphenyl)phosphonium bromide (5): Compound **4** (3.00g, 3.66 mmol) and triphenylphosphine (1.50 g, 5.72 mmol) in dry benzene (200 mL) was heated under reflux for 20 h. The product precipitated from the reaction was filtered, washed with benzene, and dried to yield pure compound **5** (3.91 g, 92.1%). ^{1}H NMR ($CDCl_3$): $\delta = 7.70$ (m, 15H), 7.33 (s, 6H), 6.90 (d, 1H), 5.85 (d, 2H); IR (KBr): $\tilde{\nu} = 1585$, 1480, 1435, 1370, 1295, 1110, 995, 840, 810, 755, 685, 495 cm^{-1}; UV/Vis (THF): λ (ε) = 305 (1530), 295 (1406), 275 (7800), 219 (140000) nm; elemental analysis calcd (%) for $C_{38}H_{18}BrCl_{14}PC_6H_6$: C 45.56, H 2.09, Br 6.89, Cl 42.79; found: C 45.44, H 2.34, Br 6.87, Cl 42.86.

Diethyl 4-[bis(2,3,4,5,6-pentachlorophenyl)methyl]-2,3,5,6-tetrachlorobenzyl phosphonate (7): A solution of the bromomethyl derivative **4** (3.00g, 3.66 mmol) in an excess of triethylphosphite (3.63 g, 21.84 mmol) were heated under reflux for 2 h at 155 °C. After this time, distilled water (25 mL) was added and the resulting mixture heated under reflux for an additional 30 min. The resulting compound was extracted with chloroform and evaporated under reduced pressure. The product was then purified by chromatography (hexanes) to yield pure compound **7** (3.2 g). ^{1}H NMR ($CDCl_3$): $\delta = 7.01$ (1H), 4.04 (q, $J = 7.10$ Hz, 4H), 3.77 (d, $J = 22.54$ Hz, 2H), 1.27 (t, $J = 7.10$ Hz, 6H); IR (KBr): $\tilde{\nu} = 2980$, 2930, 1370, 1340, 1295, 1260, 1160, 1130, 1050, 1025, 965, 805 cm^{-1}. UV/Vis (THF): λ (ε) = 302 (1170), 293 (1130), 250 (32596), 222 (105730) nm; elemental analysis calcd (%) for $C_{24}H_{13}O_3Cl_{14}P$: C 32.88, H 1.49, Cl 56.62; found C 33.03, H 1.68, Cl 56.54.

1-[Bis(2,3,4,5,6-pentachlorophenyl)methyl]-4-[2-(4-bromomethyl)ethenyl]-2,3,5,6-tetrachlorobenzene (6):

Method A: Potassium *tert*-butoxide (0.14 g, 1.28 mmol) was added to a solution of the phosphonate compound **7** (0.48 g, 0.55 mmol) in dry tetrahydrofuran (10 mL) at room temperature. The resulting yellow-orange ylide solution was stirred for 15 min. Then, 4-bromobenzaldehyde (0.13 g, 0.72 mmol) was added. The solution, which immediately turned a very intense purple color, was stirred for 1 h. The final suspension was quenched with HCl (1N, 8 mL) to give a yellowish-brown suspension that was stirred an additional hour. The resulting compound was extracted with chloroform, washed with water, and dried over sodium sulfate. The organic solvent was evaporated under reduced pressure. Pure (*E*)-**6** (0.181 g) and (*Z*)-**6** (0.228 g) were obtained by chromatography (SiO_2, chloroform/hexanes 1:1). (*E*)-**6**: ^{1}H NMR ($CDCl_3$): $\delta = 7.45$ (ABq, $J = 8.5$ Hz, 4H), 7.05 (3H, m); IR (KBr): $\tilde{\nu} = 3015$, 2925, 1635, 1590, 1535, 1490, 1405, 1365, 1340, 1295, 1240, 1140, 1075, 1010, 965, 940, 870, 805, 790, 715, 645, 532, 495 cm^{-1}; UV/Vis ($CDCl_3$): $\lambda(\cdot) = 302$ (24500), 220 (112000) nm; elemental analysis calcd (%) for $C_{27}H_7BrCl_{14}$: C 35.73, H 0.78; found C 36.40, H 1.08, Br 8.74, Cl 54.76. (*Z*)-**6**: ^{1}H NMR ($CDCl_3$): $\delta = 7.08$ (ABq, $J = 8.5$ Hz, 4H), 7.02 (s,

0947-6539/01/0701-0248 $ 17.50+.50/0 *Chem. Eur. J.* **2001**, *7*, No. 1

1H), 6.62 (ABq, $J = 12.0$ Hz, 2H); IR (KBr): $\tilde{\nu} = 3015$, 2983, 1725, 1585, 1485, 1370, 1335, 1295, 1240, 1130, 1070, 1010, 830, 805, 760, 710, 680, 655, 640, 550, 530, 460, 425 cm^{-1}; UV/Vis ($CDCl_3$): λ (ε) = 284 (13000), 221 (115000) nm; elemental analysis calcd (%) for $C_{27}H_7BrCl_{14}$: C 35.73, H 0.78; found C 35.85, H 0.78.

Method B: Potassium *tert*-butoxide (0.089 g, 0.8 mmol) was added to a solution of the phosphonium bromide **5** (0.86 g, 0.80 mmol) in dry tetrahydrofuran (20 mL) at room temperature. The resulting yellow-red ylide-type solution was stirred for 15 min. Then 4-bromobenzaldehyde (0.15 g, 0.82 mmol) was added. The solution immediately turned a very intense red color and stirring was continued for 20 h. The suspension was quenched with HCl (1N, 4 mL) to give a slightly yellowish solution that was stirred for an additional hour. Finally, water (20 mL) was added, and the mixture was extracted with chloroform. The organic layer was washed three times with water, dried over sodium sulfate, and evaporated under reduced pressure. The product was purified by chromatography (hexanes) and characterized as pure (*E*)-**6** (95%).

Bis(pentachlorophenyl)[4-(4-bromophenyl-β-styryl)-2,3,5,6-tetrachlorophenyl]methyl radical (3)

Isomer (*E*)-3: An aqueous solution of tetra *n*-butyl ammonium hydroxide (0.3 mL, 0.45 mmol) was added to a solution of compound (*E*)-**6** (0.289 g, 0.32 mmol) in dry tetrahydrofuran (5 mL) at room temperature. The resulting red-purple solution was stirred for 35 min, then *p*-chloranil (0.204 g, 0.83 mmol) was added. The resulting intensely brown solution was stirred for 1 h. After this time, the solution was evaporated to dryness and the resulting product was purified by chromatography (SiO_2, chloroform/hexanes 1:1) to yield compound (*E*)-**3** (0.270 g). IR (KBr): $\tilde{\nu} = 1630$, 1585, 1505, 1485, 1400, 1330, 965, 815, 805, 735, 710 cm^{-1}; elemental analysis calcd (%) for $C_{27}H_6BrCl_{14}$: C 35.77, H 0.67, Br 8.81, Cl 54.75; found C 35.90, H 0.49, Br 8.89, Cl 54.96.

Isomer (*Z*)-3: An aqueous solution of tetra *n*-butyl ammonium hydroxide (0.15 mL, 0.22 mmol) was added to a solution of compound (*Z*)-**6** (0.125 g, 0.14 mmol) in dry tetrahydrofuran (5 mL) at room temperature. The resulting red-purple solution was stirred for 35 min, then *p*-chloranil (0.118 g, 0.48 mmol) was added. The resulting intensely brown solution was stirred for 1 h. After this time, the solution was evaporated to dryness, and the resulting product was purified by chromatography (SiO_2, chloroform/hexanes 1:1) to yield compound (*Z*)-**3** (0.270 g). IR (KBr): $\tilde{\nu} = 1520$, 1485, 1400, 1330, 805, 735, 710 cm^{-1}; elemental analysis calcd (%) for $C_{27}H_6BrCl_{14}$: C 35.77, H 0.67, Br 8.81, Cl 54.75; found C 35.90, H 0.38, Br 8.89, Cl 54.96.

1-[Bis(2,3,4,5,6-pentachlorophenyl)methyl]-4-{(*E*)-2-{4-{(*E*)-2-{4-[bis-(2,3,4,5,6-pentachlorophenyl)methyl]-2,3,5,6-tetrachlorophenyl}ethenyl}-phenyl}ethenyl}-2,3,5,6-tetrachlorobenzene (8): Potassium *tert*-butoxide (0.075g, 0.67 mmol) was added to a solution of the phosphonium bromide **5** (0.676 g, 0.58 mmol) in dry tetrahydrofuran (15 mL) at room temperature. The resulting yellow-red ylide solution was stirred for 15 min. Then 1,4-dicarboxaldehydebenzene (0.043 g, 0.32mmol) was added, and the solution, which turned progressively purple, was stirred overnight. The final suspension was quenched with HCl (1N; 50 mL) to give a yellowish solution, which was stirred for 20 min. The resulting precipitate was filtered, washed with ethanol, H_2O, and chloroform, and was characterized as compound **8** (yield 65%). ^1H NMR (CCl_4 D_2O): $\delta = 7.25$ (s, 4H), 7.00 (m, 6H); IR (KBr): $\tilde{\nu} = 3010$, 2920, 1635, 1530, 1510, 1410, 1360, 1335, 1290, 1135, 960, 865, 800, 710, 680, 640, 525, 505 cm^{-1}; elemental analysis calcd (%) for $C_{48}H_{10}Cl_{28}$: C 36.50, H 0.63, Cl 62.86; found C 36.56, H 0.64, Cl 62.81.

(*E*,*E*)-*p*-Divinylbenzene-β,β'-ylene-bis(4-tetradecachlorotriphenylmethyl) diradical (1): An aqueous solution of tetrabutylammonium hydroxide (0.04 mL, 0.06 mmol) was added in the dark to a suspension of **8** (0.07 g, 0.24 mmol) in dry tetrahydrofuran (15 mL). The resulting purple solution was stirred for 1.5 h. After this time, an excess of *p*-chloranil (0.036 g, 0.14 mmol) was added and the stirring continued for a further 30 min. Elimination of the solvent gave a residue which was passed through silica gel (CCl_4) to give the diradical **1** as a solid, which was stable in contact with the atmosphere at temperatures up to 150 °C (yield 80%). IR (KBr): $\tilde{\nu} =$ 3025, 1624, 1510, 1330, 1255, 960, 810, 800, 800 cm^{-1}; elemental analysis calcd (%) for $C_{48}H_8Cl_{28}$: C 36.53, H 0.57, Cl 62.83; found C 36.59, H 0.62, Cl 62.86.

1-[Bis(2,3,4,5,6-pentachlorophenyl)methyl]-4-{(*E*)-2-{3-{(*E*)-2-{4-[bis-(2,3,4,5,6-penta-chlorophenyl)methyl]-2,3,5,6-tetrachlorophenyl}ethenyl}-phenyl}ethenyl}-2,3,5,6-tetrachlorobenzene (9): Potassium *tert*-butoxide (0.163 g, 1.4 mmol) was added to a solution of the phosphonium bromide **5** (1.19 g, 1.026 mmol) in dry tetrahydrofuran (30 mL) at room temperature. The resulting yellow-red ylide solution was stirred for 15 min, then 1,3-dicarboaldehydebenzene (0.08 g, 0.6 mmol) was added. The solution, which turned progressively wine-red, was stirred for 16 h. The final suspension was quenched with HCl (1N, 20 mL) to give a yellowish solution that was stirred for 20 min. The resulting precipitate was filtered, washed with ethanol, H_2O, and chloroform, and characterized as compound **9** (yield 61%). ^1H NMR ($CDCl_3$): $\delta = 7.67$ (m, 1H), 7.53 (m, 3H), 7.12 (m, 4H), 7.07 (s, 2H); IR (KBr): $\tilde{\nu} = 3010$, 2920, 1640, 1535, 1520, 1365, 1340, 1295, 1240, 1135, 960, 860, 808, 715, 680, 645, 530, 495 cm^{-1}; elemental analysis calcd (%) for $C_{48}H_{10}Cl_{28}$: C 36.50, H 0.63, Cl 62.86; found C 36.63, H 0.47, Cl 62.50.

(*E*,*E*)-*m*-Divinylbenzene-β,β'-ylene-bis(4-tetradecachlorotriphenylmethyl) diradical (2): An aqueous solution of tetrabutylammonium hydroxide (0.07 mL, 0.08 mmol) was added in the dark to a suspension of **9** (0.09 g, 0.32 mmol) in dry tetrahydrofuran. The resulting purple solution was stirred for 1.5 h. After this time, an excess of *p*-chloranil (0.024 g, 0.09 mmol) was added and the stirring continued for 30 min. Elimination of the solvent gave a residue which was passed through silica gel (CCl_4) to give the diradical **2**, which was obtained as a solid that was stable in contact with the atmosphere at temperatures up to 150 °C (yield 68%). IR (KBr): $\tilde{\nu} = 2920$, 1510, 1340, 1260, 960, 815, 780, 755 cm^{-1}; elemental analysis calcd (%) for $C_{48}H_8Cl_{28}$: C 36.53, H 0.57, Cl 62.83; found C 37.20, H 0.53, Cl 62.27.

Acknowledgments

This work was supported from DGES (PB96–0862-C02–01), CIRIT (1998SGR-96–00106) and the 3MD Network of the TMR program of the E.U. (contract ERBFMRXCT 980181). D.R.-M. is grateful to the Generalitat de Catalunya for a postdoctoral grant.

[1] a) A. Harriman, R. Ziessel, *Coord. Chem. Rev.* **1998**, *171*, 331; b) M. N. Paddon-Row, *Acc. Chem. Res.* **1994**, *27*, 18; c) M. R. Wasielewski, *Chem. Rev.* **1992**, *92*, 435.

[2] Typical molecular-sized systems would permit the use of $\approx 10^{13}$ logic gates per cm^2 compared with the present capacity of a microchip of less than 10^8 gates per cm^2, thereby offering a 10^5 decrease in required size. In addition, the response times of molecular devices can be in the range of femtoseconds, while the fastest current devices operate in the nanosecond regime: a) J. M. Tour, M. Kozaki, J. M. J. Seminario, *J. Am. Chem. Soc.* **1998**, *120*, 8486; b) J. M. Seminario, J. M. Tour in *Molecular Electronics-Science and Technology* (Eds.: A. Aviram, M. A. Ratner), New York Academy of Science, New York, **1998**, p. 69.

[3] J.-P. Sauvage, J.-P. Collin, J.-C. Chambron, S. Guillerez, C. Coudret, *Chem. Rev.* **1994**, *94*, 993.

[4] See for instance: a) R. J. Crutchley, *Adv. Inorg. Chem.* **1994**, *41*, 273; b) C. Creutz, *Prog. Inorg. Chem.* **1983**, *30*, 1.

[5] a) S. F. Nelsen, H. Q. Tran, M. A. Nagy, *J. Am. Chem. Soc.* **1998**, *120*, 298; b) S. F. Nelsen, M. R. Ramm, J. J. Wolf, D. R. Powell, *J. Am. Chem. Soc.* **1997**, *119*, 6863; c) K. Lahlil, A. Moradpour, C. Bowlas, F. Menou, P. Cassoux, J. Bonvoisin, J. P. Launay, G. Dive, D. Dehareng, *J. Am. Chem. Soc.* **1995**, *117*, 9995; d) J. Bonvoisin, J. P. Launay, M. Van der Auweraer, F. C. De Schryver, *J. Phys. Chem.* **1994**, *98*, 5052; e) S. F. Rak, L. L. Miller, *J. Am. Chem. Soc.* **1992**, *114*, 1388; f) S. Utamapanya, A. Rajca, *J. Am. Chem. Soc.* **1991**, *113*, 9242; g) J. P. Telo, C. B. L. Shohoji, B. Herold, G. Grampp, *J. Chem. Soc. Faraday Trans.* **1992**, *88*, 47; h) F. Gerson, T. Wellauer, A. M. Oliver, M. N. Paddon-Row, *Helv. Chim. Acta* **1990**, *73*, 1586; i) M. Ballester, I. Pascual, J. Riera, J. Castañer, *J. Org. Chem.* **1991**, *56*, 217.

[6] a) M. Ballester, J. Riera, J. Castañer, A. Rodríguez, *Tetrahedron Lett.* **1971**, 2079; b) M. Ballester, J. Riera, J. Castañer, J. Veciana, C. Rovira, *J. Org. Chem.* **1982**, *47*, 4498; c) M. Ballester, *Acc. Chem. Res.* **1985**, *297*, 131; d) J. Veciana, J. Riera, J. Castañer, N. Ferrer, *J. Organomet. Chem.* **1985**, *297*, 131; e) O. Armet, J. Veciana, C. Rovira, J. Riera, J.

Castañer, E. Molins, J. Rius, C. Miravitlles, S. Olivella, J. Brichfeus, *J. Phys. Chem.* **1987**, *91*, 5608, and references cited therein.
[7] J. Sedo, D. Ruiz, J. Vidal-Gancedo, C. Rovira, J. Bonvoisin, J.-P. Launay, J. Veciana, *Adv. Mater.* **1996**, *8*, 748.
[8] V. Grosshenny, A. Harriman, R. Ziessel, *Angew. Chem.* **1995**, *107*, 1211; *Angew. Chem. Int. Ed. Engl.* **1995**, *34*, 1100, and references therein.
[9] a) C. Patoux, J.-P. Launay, M. Beley, S. Chodorowski-Kimmes, J.-P. Collin, S. James, J.-P. Sauvage, *J. Am. Chem. Soc.* **1998**, *120*, 3717; b) F. Barigelletti, L. Flamigni, V. Balzani, J.-P. Collin, J.-P. Sauvage, E. C. Constable, A. M. W. Cargill1 Thompson, *J. Chem. Soc. Chem. Commun.* **1993**, 942; F. Barigelletti, L. Flamigni, V. Balzani, J.-P. Collin, J.-P. Sauvage, A. Sour, E. C. Constable, A. M. W. Cargill1 Thompson, *J. Am. Chem. Soc.* **1994**, *116*, 7692; c) A. C. Benniston, V. Goulle, A. Harriman, J. M. Lehn, B. Marczinke, *J. Phys. Chem.* **1994**, *98*, 7798.
[10] In order to optimize the intramolecular electron-transfer rates between two terminal radicals, the synthesis of the bridge requires the use of molecular units with highly restricted conformational mobility, high solubility, and high thermal and electrochemical stabilities: "Atomic and Molecular Wires", A. Gourdon *NATO ASI Ser. E: Applied Sciences*, **1997**, *198*, 89.
[11] Preliminary results have already been presented in a communication: J. Bonvoisin, J.-P. Launay, C. Rovira, J. Veciana, *Angew. Chem.* **1994**, *106*, 2190; *Angew. Chem. Int. Ed. Engl.* **1994**, *33*, 2106.
[12] R. Ziessel, M. Hissler, A. El-Ghayoury, A. Harriman, *Coord. Chem. Rev.* **1998**, *178–180*, 1251.
[13] M. Ballester, J. Veciana, J. Riera, J. Castañer, C. Rovira, O. Armet, *J. Org. Chem.* **1986**, *51*, 2472.
[14] For other strongly (*E*)-selective reactions, see for example: H. Pommer, A. Nurenbach, *Angew. Chem.* **1977**, *89*, 437; *Angew. Chem. Int. Ed. Engl.* **1977**, *16*, 423.
[15] H. O. House, *Modern Synthetic Reactions*, 2nd ed., Benjamin, Menlo Park, **1972**, p. 608.
[16] a) K. Wurst, O. Elsner, H. Schottenberger, *Synlett* **1995**, 833; b) J.-G. Rodríguez, A. Oñate, R. M. Martin-Villamil, I. Fonseca, *J. Organomet. Chem.* **1996**, *513*, 71.
[17] L. Fitjer, U. Quabeck, *Synth. Commun.* **1985**, *15*, 855.
[18] For a review see: J. Stec, *Acc. Chem. Res.* **1983**, *16*, 411.
[19] It is well known that molecules of the type Ar_3Z, in which three aryl groups (Ar) are bonded to a central Z atom and which have a sp^2 hybridization, are propeller-like in shape. A large number of theoretical studies on the stereochemistry of these propeller-like systems were performed by Mislow et al. (K. Mislow, *Acc. Chem. Res.* **1976**, *9*, 26). They demonstrated that in the most simple cases, where the three aryl groups (blades) are either not substituted or else are symmetrically substituted around the C_{ar}–Z bond axis of each aryl group (i.e., groups having local C_2 axes), the molecule always has at least two enantiomeric forms owing to the intrinsic stereogenic center (helicity) of any propeller that gives chirality to the molecule. If the helix adopts a clockwise sense the enantiomer is called *Plus* (*P*), whereas if it adopts the opposite sense is called *Minus* (*M*). For diradicals **1** and **2** it is easy to predict the existence of three stereoisomers: one pair of enantiomers—namely (*P*,*P*) and (*M*,*M*)—and a *meso* form—namely (*M**,*P**)—due to the presence of two triphenylmethyl stereogenic centers. (N. Ventosa, D. Ruiz-Molina, J. Sedó, C. Rovira, X. Tomas, J.-J. André, A. Bieber, J. Veciana, *Chem. Eur. J.* **1999**, *5*, 3533). Semiempirical calculations were done by using initial input molecules that had one of the triphenylmethyl units in the *M* form and the other in the *P* form. It was also checked that the use of another stereoisomer did not have any influence on the final minimized geometries.
[20] It is well known that the unpaired electron of highly chlorinated triphenylmethyl radicals and the negative charge of the corresponding carbanions are mainly localized on the alpha carbons (see ref. [6], and references cited therein). Therefore, the two alpha carbon atoms of **1** and **2** can be considered, in a first approximation, as the *electron active sites* for the electron-transfer phenomena. It should also be considered that the distance between the electron active sites may change from one conformer to the other. For instance, the through-space distance between the electron active sites for diradical **2** ranges from 16.9 to 15.1 Å along the different conformational isomers obtained simply by rotating the single bond that connects the central phenylene unit and one of the vinylene moieties.
[21] A. Hradsky, B. Bildstein, N. Schuler, H. Schottenberger, P. Jaitner, K.-H. Ongania, K. Wurst, J.-P. Launay, *Organometallics* **1997**, *16*, 392.
[22] No differences in the magnetic behavior of (*E*)-**3** and (*Z*)-**3** were noticed.
[23] S. D. McGlynn, T. Azumi, M. Kinoshita in *Molecular Spectroscopy of the Triplet State*, PrenticeHall, New Jersey, **1969**.
[24] A.-C. Ribou, J.-P. Launay, K. Takahashi, T. Nihira, S. Tarutani, C. W. Spangler, *Inorg. Chem.* **1994**, *33*, 1325.
[25] S. F. Nelsen, S. C. Blacstock, Y. Kim, *J. Am. Chem. Soc.* **1987**, *109*, 677.
[26] MOPAC 93.00, a) J. J. Stewart, M. J. S. Dewar, E. G. Zoebish, E. F. Healy, *J. Am. Chem. Soc.* **1985**, *107*, 3902; b) M. J. S. Dewar, E. G. Zoebish, *J. Mol. Struct.(Theochem)* **1988**, *180*, 1.
[27] The variation of the intervalence absorption band versus the average reduction state can be used to determine the comproportionation constant, K_c, according to Equation (6). In the present case, the resulting value of K_c is 7. This value is employed in Equation (7) for the calculation of the corrected spectra.

$$K_c = [\mathbf{1}^{\bullet-}]^2/[\mathbf{1}][\mathbf{1}^{2-}] \quad (6)$$

$$\varepsilon(\mathbf{1}^{\bullet-}) = \left[\frac{2 + \sqrt{K_c}}{\sqrt{K_c}}\right]\varepsilon(\mathbf{1}^{\bullet-})_{app} - \frac{\varepsilon(\mathbf{1}^{\bullet\bullet}) + \varepsilon(1^{2-})}{\sqrt{K_c}} \quad (7)$$

Here $(\mathbf{1}^{-})$ and $(\mathbf{1}^{-})_{app}$ are the true and the apparent extinction coefficients of the radical anion $\mathbf{1}^{\bullet-}$, and $(\mathbf{1}^{\bullet})$and $(\mathbf{1}^{2-})$ are the extinction coefficients of diradical **1** and dianion $\mathbf{1}^{2-}$, respectively. Band deconvolution of the corrected spectrum of $\mathbf{1}^{\bullet-}$ was performed by assuming Gaussian profiles in order to separate the intervalence band from other nearby bands (see Figure 4). This deconvolution procedure has already been described in ref. [24] and has the advantage of giving a better estimate of the Marcus λ value.

[28] J. Heinzer, *J. Mol. Phys.* **1971**, *22*, 167; *Quantum Chemistry Program Exchange* **1972**, N° 209.
[29] S. F. Nelsen, R. F. Ismagilov, D. A. Trieber II, *Science* **1997**, *278*, 846.
[30] O. Elsner, D. Ruiz-Molina, J. Vidal-Gancedo, C. Rovira, J. Veciana, *Chem. Commun.* **1999**, 579.
[31] C. Patoux, C. Coudret, J. P. Launay, C. Joachim, A. Gourdon, *Inorg. Chem.* **1997**, *36*, 5037.
[32] a) M. J. Shephard, M. N. Paddon-Row, K. D. Jordan, *J. Am. Chem. Soc.* **1994**, *116*, 5328; b) M. N. Paddon-Row, *Acc. Chem. Res.* **1994**, *27*, 18, and references cited therein.
[33] M. J. S. Dewar, E. G. Zoebisch, E. F. Healy, J. J. P. Stewart, *J. Am. Chem. Soc.* **1985**, *107*, 3902.

Received: March 15, 2000
Revised version: August 3, 2000 [F2367]

  0947-6539/01/0701-0250 $ 17.50+.50/0